19th International Conference
ENGINEERING MECHANICS 2013
Svratka, Czech Republic, May 13 – 16, 2013

A CALIBRATION OF GURON-TVERGAARD-NEEDLEMAN MICROMECHANICAL MODEL OF DUCTILE FRACTURE

L. Stratil[*], H. Hadraba[**], F. Šiška[***], I. Dlouhý[****]

Abstract: *Fracture mechanics characteristics of ductile fracture often depend on geometry and size of specimens. A micromechanical modelling of material damage proposes a tool for treatment of geometry and size effects in fracture mechanics. Application of micromechanical model for certain material requires a calibration of model's parameters. This contribution presents the calibration procedure of Gurson-Tvergaard-Needleman model of ductile fracture for Eurofer97 steel. The identification of ductile damage of the steel and its tensile properties at various level of stress triaxiality by testing smooth and notched bars were determined in the previous study. The calibration procedure was performed by hybrid method as a combination of FEA simulations of tensile tests and fractography analyses. The Gurson-Tvergaard-Needleman model performance is greatly influenced by true stress-true strain curve of the material. It was verified that derivation of true stress-true strain curve of the material by using of multiple linear regression model proposed by Mirone is very suitable.*

Keywords: ***ductile fracture, GTN model, void nucleation, MLR model, Eurofer97***

1. Introduction

It is usually observed that R-curves, as fracture mechanics characteristics of resistance against stable crack growth, of tested geometries depend on size, geometry and configuration of specimens without no general trend (Wallin et al., 2002, Lucon & Scibetta, 2009). One possibility to deal with size and geometry effects offers local approach to fracture, which goes beyond the limits of conventional fracture mechanics. Application of local approach to fracture involves identification of damage micromechanism of the material, choice and calibration of suitable micromechanical model of damage. One of the most using micromechanical models of ductile fracture in fracture mechanics is the Gurson-Tveergard-Needleman (GTN) model (Tvergaard & Needleman, 1984). In the previous study (Stratil et al., 2012) obtained parameters of GTN model based on smooth tensile specimen results were not sufficiently determined. This contribution continues with determination of micromechanical parameters of GTN model based on both smooth and notched tensile results.

2. Gurson-Tvergaard-Needleman model

The Gurson model describes the plasticity of material via behaviour of voids in ideal-plastic Mises material (Gurson, 1977). Because of some discrepancies of original Gurson model in comparison with experimental results, it was modified by Tvergaard (1981, 1982) and later by Needleman & Tvergaard (1984). This modification modification is called Gurson-Tvergaard-Needleman model. The yield function of the GTN model has the following form:

[*] Ing. Luděk Stratil: Institute of Physics of Materials, ASCR, Žižkova 22; 616 62, Brno; CZ, e-mail: stratil@ipm.cz and Institute of Material Science and Engineering, Faculty of Mechanical Engineering, Brno University of Technology, Technická 2896/2; 616 69, Brno; CZ, e-mail: ystrat04@stud.fme.vutbr.cz

[**] Ing. Hynek Hadraba, Ph.D.: Institute of Physics of Materials, ASCR, Žižkova 22; 616 62, Brno; CZ, e-mail: hadraba@ipm.cz

[***] Dr. Ing. Filip Šiška, Ph.D.: Institute of Physics of Materials, ASCR, Žižkova 22; 616 62, Brno; CZ, e-mail:siska@ipm.cz

[****] Prof. Ing. Ivo Dlouhý, CSc.: Institute of Physics of Materials, ASCR, Žižkova 22; 616 62, Brno; CZ, e-mail: idlouhy@ipm.cz and Institute of Material Science and Engineering, Faculty of Mechanical Engineering, Brno University of Technology, Technická 2896/2; 616 69, Brno; CZ, email: dlouhy@fme.vutbr.cz

$$\phi(q,\overline{\sigma},f,\sigma_m)=\frac{q^2}{\overline{\sigma}^2}+2q_1 f^*\cosh\left(\frac{3q_2\sigma_m}{2\overline{\varsigma}}\right)-1-\left(q_1 f^*\right)^2=0, \tag{1}$$

where f is the void volume fraction, σ_m is the mean normal stress, q is conventional von Mises equivalent stress, $\overline{\sigma}$ is the flow stress of the matrix material, q_1, q_2 are constants introduced by Tvergaard (1981, 1982). The function $f^*(f)$ was applied by Needleman & Tvergaard (1984) to model rapid loss of the material stress-carrying capacity after the occurrence of void coalescence as observed during the test. This function is expressed as follows:

$$f^* = f \text{ for } f < f_c \tag{2}$$

$$f^* = f_c + \frac{f_u^* - f_c}{f_f - f_c} \text{ for } f \geq f_c, \tag{3}$$

where $f_u^* = 1/q_1$. The complete loss of load-carrying capacity occurs at $f = f_F$ i.e. ultimate void volume fraction. The function becomes more predominant once the void volume fraction f exceeds a critical value f_c.

The increase in void volume fraction consists of two terms: the nucleation of new voids and growth of existing voids. It can be written as:

$$\Delta f = \Delta f_{nucl} + \Delta f_{gr}. \tag{4}$$

The symbol Δ represents the increment in the quantity.

The GTN model can simulate microvoid nucleation, growth and by introducing empirical void coalescence criterion the void coalescence. For existing voids the model can describe the softening effect caused by the voids on material behaviour and at the same time can predict the void growth rate during plastic deformation. Different materials may have different nucleation laws as a claster model (parameter representing initial void volume fraction, f_0) and continuous or statistical void nucleation model. Parameters q_1 and q_2 describe growth of voids, parameters ε_n and s_n together with f_n (parameter representing amount of nucelated fraction of voids, f_n) describe the statistical nucleation model. For material, where neither one of models is suitable, complex model consisting of their combination should be used. Because the laws describing voids growth and nucleation cannot itself treat void coalescence, the complete Gurson models contains one empirical treatment of it called critical volume fraction (f_c). The coalescence occurs via faster growth rate when a critical void volume fraction has been reached. The void coalescence will be finished (material load carrying capacity becomes zero) when the void volume fraction reaches another value – the volume fraction at final failure (f_f).

The ductile behaviour of the material is described by its true stress-strain curve and ductile damage behaviour is in case of GTN model characterized by eight parameters: q_1, q_2, f_0, ε_n, s_n, f_n, f_c and f_f.

Different ways can be followed for identification of GTN model parameters: fully phenomenological method, i.e. determination of the damage parameters from macroscopic mechanical response (He et al., 1998), unit cell numerical computation (Faleskog et al., 1998), fractography and metallography analysis (Berdin & Haušild, 2002), (ESIS, 1992), or direct damage kinetics assessment (Berdin & Haušild, 2002). Any combination of these three methods can be also used.

3. Experimental

3.1. Derivation of input material curve

The results of tensile testing were taken from study Stratil et al., 2012, where testing of smooth and notched tensile bars was performed. Two pieces of specimens per geometry had been tested. The smooth tensile specimens and specimens with notch radii 3 mm and 1 mm had been prepared to have the same initial diameter 4 mm and gauge length 20 mm. The specimens were tested quasistatically by the speed 1 mm/min at room temperature. During the tests axial displacement of specimens was monitored by the external extensometer, the actual diameter was monitored optically by digital camera in regular intervals. With increasing stress triaxiality in the specimen centre, the stress characteristics increase and deformation characteristics decrease, Fig. 1. The information about diameter reduction was used for determination of true stress-true strain curves of all tensile specimens, Fig. 1.

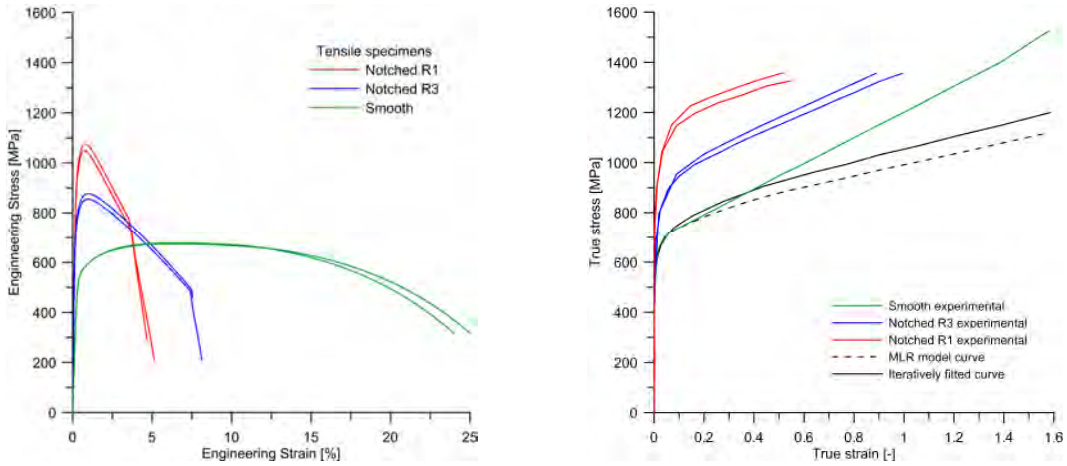

Fig. 1: Experimental curves engineering stress- strain for tensile specimens (left) and corresponding curves true stress-strain obtained from actual load and diameter reduction (right).

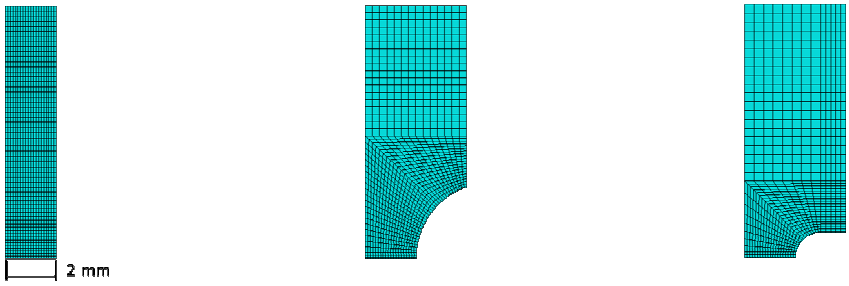

a) smooth b) notched, R=3 mm c) notched, R=1 mm

Fig. 2: 2D asisymmetric models of tensile specimens with element size 0.1×0.1 mm.

The input of material properties into FEA software ABAQUS requires description of true stress-strain curve as pairs of material data true stress and plastic true strain. For relevant behaviour of FE model at large deformation levels, the true stress-strain curve have to be described up to large deformations about 200-300 %. The true stress σ_t and true strain ε_t can be derived from round tensile test bars data in the region of uniform deformation of tensile test up to onset of necking:

$$\sigma_t = F/(\pi \cdot r^2) \approx \sigma_e(1+\varepsilon_e) \tag{5}$$

$$\varepsilon_t = 2 \cdot \ln(r_0/r) \approx \ln(1+\varepsilon_e), \tag{6}$$

where F is actual load, r_0 and r are initial and actual radius of specimen cross section, respectively, σ_e and ε_e are equivalent von Mises stress and strain, respectively. The curve so obtained, usually identified as the "true-stress (σ_t) true strain (ε_t) curve" characterizes correctly the material only in the pre-necking phase of the straining. During the post-necking phase this curve differs substantially from the real material curve $\sigma_e(\varepsilon_e)$ because, since the necking phenomenon arises, the stress state departs fradually from uniaxiality and from uniformity across the neck section. As a result, the experimentally determined curve true stress-strain from smooth tensile test in Fig. 1 is not suitable as input into FE software especially in case of detailed simulation of tensile specimen responses load vs. diameter reduction. In order to get proper definition of true stress-strain curve, two approaches were chosen. First was based on iteration trial-error fitting procedure of true stress-strain curve of smooth tensile specimen in necking region. Up to neck formation the true stress and strain were determined according to equations (5) and (6). For purposes of modelling, 2D axisymmetric models of tested tensile specimen were created in ABAQUS software, Fig. 2. Models were built from elements CAX4R of size 0.1 x 0.1 mm and were displacement driven in regime of large deformations in Explicit module. The suitable form of true stress-strain curve was derived after more than forty iterations until sufficient response of load vs. elongation an load vs. diameter of all tensile bars were achieved, Fig. 3. The derived curve is shown in Fig. 1.

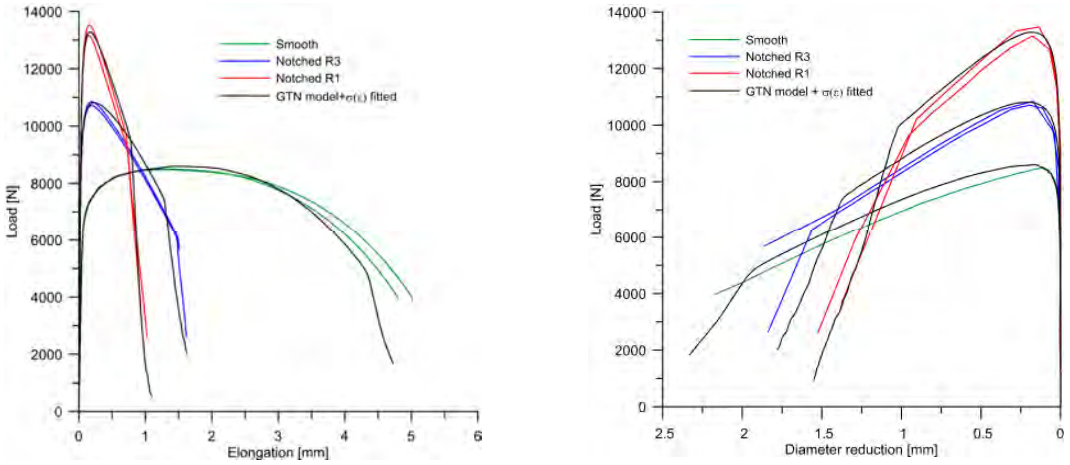

Fig. 3: Comparison of experimental and computed response of tensile specimens load vs. elongation (left) and load vs. diameter reduction (right) for fitted true stress-strain curve.

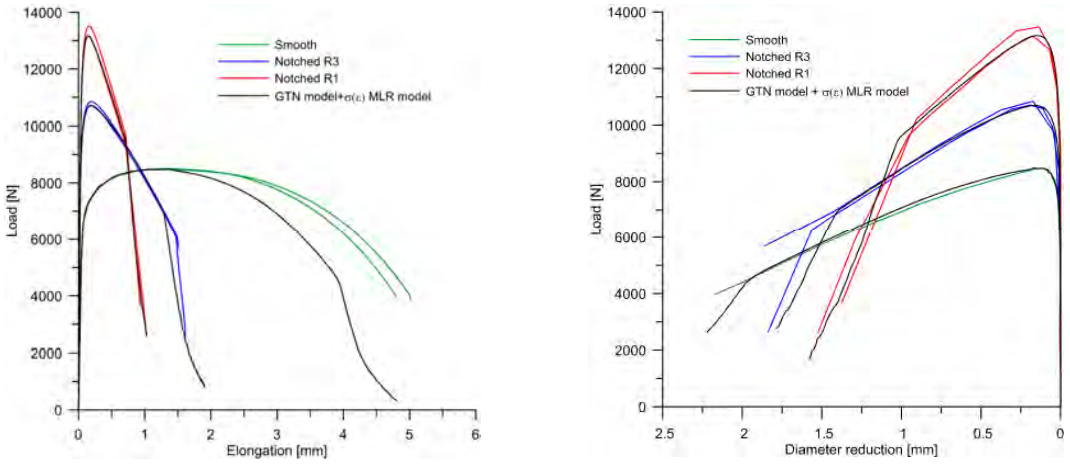

Fig. 4: Comparison of experimental and computed response of tensile specimens load vs. elongation (left) and load vs. diameter reduction (right) for true stress-strain curve of MRL model.

The second approach was based on application of multilinear regression model (MLR) proposed by Mirone (Mirone, 2004), which is based on experimental and numerical observation of neck formation of many metal engineering materials. The perturbing effects of the necking phenomenon on the stress and strain distribution had been found to be almost material-independent. The only material-dependence consists of the plastic strain value which triggers the whole necking initiation, ε_N . The equivalent von Mises stress in necking region is in MRL model given by:

$$\sigma_{t\_MRL} = F/(\pi \cdot r^2) \cdot MLR_\sigma(\varepsilon_e - \varepsilon_N), \tag{7}$$

where function MLR_σ is the fourth order polynomial able to fit the axial stresses in necking part of metal engineering alloys studied. In this study the MLR_σ was taken as coefficient by which the true stress σ_t was corrected after necking initiation of smooth tensile test. The resulted curve is shown in Fig. 1. This curve describes very well the responses of load vs. diameter and load vs. elongation for all tested specimens with the exception of load vs. elongation response for smooth specimen, Fig. 4. This can be neglected as load vs. elongation response of smooth tensile specimen is not very sensitive to localized deformation during necking formation. The iteratively fitted curve of true stress-strain and curve derived from MRL model is quite similar. So both approaches lead to similar definition of material input curve for FE modelling and they are thus suitable for modelling of material behaviour at large deformation levels.

3.2. Calibration of GTN model parameters

In this study hybrid methodology calibration of parameters of GTN model was carried out as a combination of fractography and metallography examinations and FE analysis. The identification of damage micromechanism of the Eurofer97 steel was also carried out within the study Stratil et al. 2012. Ductile damage identification of the Eurofer97 steel was carried out by fractography analysis of fracture surfaces of broken tensile specimens and by metallographic examination of central parts of broken tensile bars along their longitudinal axis. The quantitative voids measurements were obtained by processing the images from area of interest using image analysis as shown in Fig. 5. The examination revealed that voids nucleate just in the neck region in small distance from the fracture surfaces and any voids were observed neither in uniformly deformed part of smooth specimen nor in larger distance from notch tip of specimens with radii. The damage process of the steel is driven by the voids' nucleation and their subsequent growth. No marks of significant coalescence process were observed under the fracture surfaces suggesting that the void coalescence was not acted during the substantial part of damage evolution. Voids nucleate preferentially at the largest precipitates by mechanism of decohesion matrix/particle. As the stress triaxiality in specimens centre increase in sence of smooth, notched specimen with radius 3 mm and 1 mm, it causes larger growth of voids, which is promoted at the expense of growth nucleation probably as reason of lower deformation level. The average representative value of void volume fraction from areas below the fracture surfaces was determined as 0.0045.

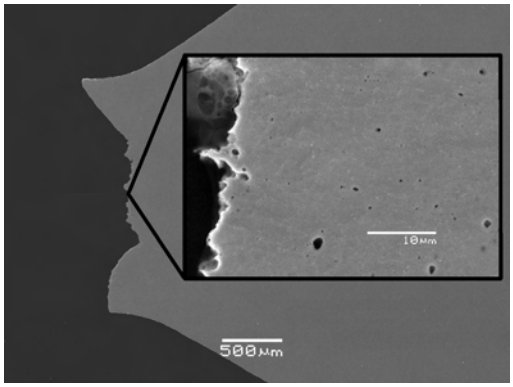

Fig. 5: The detail of analysed area under the fracture surface of notch specimen, R=3mm.

The results of metallography and fractography analyses were used for establishment methodology for calibration of GTN parameters. Because of observation of voids just in close distance to fracture surface and any observation of voids in uniformly deformed part of smooth specimen or areas in larger distance from the notch tip of specimens with radii, the value of initial void volume fraction f_0 was set zero. Next the obtained value of void volume fraction from areas below the fracture surfaces was set as critical void volume fraction f_c. Just the process of nucleation and growth of void was taken into account. Parameters of ε_n and s_n were set as their usual values recommended by Tvergaard (1981, 1982), respectively and the values of parameters q_1 and q_2 were taken as optimized values based on cell computation in work of Faleskog et al., 1998, Tab. 1. The values of remaining parameters f_n and f_f were fitted by performing parametric studies of all tested tensile specimens in Fig. 3, 4 and Tab. 1. The same models of tensile specimens as described above were used for this calibration procedure.

Tab. 1: The identified parameters of GTN model for Eurofer97 steel.

q_1	q_2	ε_n	s_n	f_n	f_0	f_c	f_f
1.46	0.931	0.3	0.1	0.00055	0	0.0045	0.1

4. Discussion

The identified parameters of GTN model are slightly different from that ones determined in previous study (Stratil et al., 2012). The values of q_1 and q_2 used in present study are believed to be more optimal then their basic values previously applied ($q_1 = 1.5$ and $q_2 = 1.0$), as they were taken for model material with similar yield strength and hardening behaviour as Eurofer97 steel. The values of f_n, f_c and f_f are also lower in comparison with prior calibrated values. This is explained by the lower average value of void volume fraction from areas below the fracture surfaces, which was determined from more detailed analysis of smooth and notched specimens. The value of $f_c = 0.0045$ is believed to be well representative for studied steel. Concerning currently calibrated values of f_n and f_f, it must be noted that calibrated values of these parameters are phenomenological, as they were fitted to macroscopic response of tensile specimens. But on the other hand, the set of obtained GTN parameters gives the good comparison to tensile tests results for both identified material curves. However, in comparison with results of previous study the biggest difference was found in definition of material curve of the steel. In previous study the determination of this curve was made just using results of smooth tensile specimen load vs. elongation. This information itself is not very suitable for determining of material true stress-strain curve as the elongation is not very sensitive for description of deformation behaviour during necking phase of the test. On the other hand such test can be used for calibration of relevant true stress-strain curve using MRL model. Generally, the knowledge of dependence load vs. diameter reduction during tensile test or necessity of results from notched tensile specimens for reliable calibration GTN model parameters is needed.

Next issue connected with micromechanical modeling is the basic volume of damage, often described as the length scale. This parameter can be reasonably connected with microstucture of the material (Berdin, C. & Haušild, P. (2002)). In FEA the length scale is usually directly connected with the element size at the crack or notch tip. However, in this study the calibration process and all simulations were done with fixed element size 0.1×0.1 mm, so the obtained set of GTN model parameters is calibrated for this element size. Lower or higher element sizes enhance or weaken the process of simulated damage.

5. Conclusions

The calibration of micromechanical parameters of Gurson-Tvergaard-Needelman model of ductile fracture was performed by combination of tensile bars testing and its numerical simulation. Calibrated

values of micromechanical parameters were based on the results of quantitative study of void nucleation and growth from previous study and on the results of parametric studies of chosen micromechanical parameters. The successful calibration of micromechanical parameters requires at least determination of dependence load vs. diameter diameter reduction during tensile test of smooth specimen. Performance of Gurson-Tvergaard-Needelman model also depends on true stress-true strain curve of the material. This curve can be easily derived according to the model proposed by Mirone from results of smooth tensile bar or by its fitting to the results of smooth and notched tensile bars. The obtained parameters of GTN model together with true stress-strain curve for Eurofer97 steel will be used for description and prediction of size effect on J-R curves of three-point-bend specimens

Acknowledgement

The authors gratefully thank for the financial support of projects of the Operational Programme "Education for Competitiveness" No. CZ.1.07/2.3.00/20.0197 and the project of specific research FSI-J-12-27/1733.

References

Berdin, C. & Haušild, P. (2002) Damage mechanisms and local approach to fracture, Part I: Ductile fracture, in*: Proc. Transferability of Fracture Mechanical Characteristics* (I. Dlouhý ed), Kluwer Academic Publishers, Netherlands, pp.167-180.

ESIS Procedure for Determining the Fracture Behaviour of Materials, ESIS P2-92, Delft, 1992.

Faleskog, J., Gao, X. & Shih, C.F. (1998) Cell model for nonlinear fracture mechanics-I micromechanics calibration. International Journal of Fracture, 89, pp. 355-373.

Gurson, A.L. (1977) Continuum theory of ductile rupture by void nucleation and growth. Part 1-yield criteria and flow stress for porous ductile media. *Journal of Engineering Materials and Technology*, 99, pp. 2-15.

He, R., Steiglich, J., Heerens, J., Wang, G. W., Brocks, W. & Dahms, M. (1998) Influence of particle size and volume fraction on damage and fracture in Al-A13Ti composites and micromechanical modeling using the GTN model, *Fatigue and Fracture of Engineering Materials*, 21 pp. 1189-1201.

Lucon, E. & Scibetta, M. (2009) Miniature compact tension specimen for upper shelf toughness measurements on RPV steels, in*: Proc. 5th Small specimen test technique, STP 1502* (M.Sokolov eds), ASTM Int., West Conshohocken, pp.18-31.

Mirone, G. (2004) A new model for the elastoplastic characterization and the stress-strain determination on the necking section of a tensile specimen. *International Journal of Solids and Structures,* 41, pp. 3545-3564.

Stratil, L., Hadraba, H., Kozák, V., Dlouhý, I. (2012) Modelling of ductile fracture for sub-sized three-point-bend geometry, in*: Proc. 18th Int.Conf. Enginnering Mechanics 2012* (J.Náprstek & C.Fischer eds), Inst. Of Theor. and Applied Mechanics, Prague, pp.1253-1258.

Stratil, L., Hadraba, H., Dlouhý, I. (2012) Ductile damage identification and tensile notch effect for Eurofer97 steel. *Acta Metallurgica Slovaca-Conference,* 3, pp. 185-190.

Tvergaard, V. & Needleman, A. (1984) Analysis of the cup-cone fracture in a round tensile bar. *Acta Metallurgica*, 32, pp.157-169.

Tvergaard, V. (1981) Influence of voids on shear band instabilities under plane strain conditions. *International Journal of Fracture*, 17, pp. 389-407.

Tvergaard, V. (1982) On localization in ductile materials containing spherical voids. *International Journal of Fracture*, 18, pp.237-252.

Wallin, K., Laukkanen, A., & Tähtinen, S. (2002) Examination of fracture resistance of F82H steel and performance of small specimen in transition and ductile regimen, in*: Proc. 4th Small specimen test technique, STP 1418* (M.Sokolov, J.D. Landes & G.E. Lucas eds), ASTM Int., West Conshohocken, pp.33-47.